Boost Converter Fed High Performance BLDC Drive for Solar PV Array Powered Air Cooling System

Shobha Rani DEPURU[1], Muralidhar MAHANKALI[2]

[1]Department of Electrical and Electronics Engineering, Institute of Aeronautical Engineering, Jawaharlal Nehru Outer Ring Road, Dundigal, Hyderabad, Telangana 500043, India
[2]Department of Electrical and Electronics Engineering, Sri Venkateswara University College of Engineering, Tirupati 517502, Andhra Pradesh, India

depuru_shobha@yahoo.com, muralidhar6666@gmail.com

Abstract. *This paper proposes the utilization of a DC-DC boost converter as a mediator between a Solar Photovoltaic (SPV) array and the Voltage Source Inverters (VSI) in an SPV array powered air cooling system to attain maximum efficiency. The boost converter, over the various common DC-DC converters, offers many advantages in SPV based applications. Further, two Brushless DC (BLDC) motors are employed in the proposed air cooling system: one to run the centrifugal water pump and the other to run a fan-blower. Employing a BLDC motor is found to be the best option because of its top efficiency, supreme reliability and better performance over a wide range of speeds. The air cooling system is developed and simulated using the MATLAB/Simulink environment considering the steady state variation in the solar irradiance. Further, the efficiency of BLDC drive system is compared with a conventional Permanent Magnet DC (PMDC) motor drive system and from the simulated results it is found that the proposed system performs better.*

Keywords

Boost converter, brushless DC motor, permanent magnet DC motor, solar irradiance, solar photovoltaic array, voltage source inverter.

1. Introduction

Over recent years, renewable energy sources have become an indispensable part of world energy consumption. Among all the available renewable energy sources, solar energy is regarded as the most viable source of energy since it is abundantly available [1], [2] and [3]. India has an average annual temperature that ranges from 25–27.5 °C which means that India has huge solar potential. Although several researches have been carried out on SPV array fed automotive and irrigation systems combining various DC-DC converters and motor drives, very less work has been done on Photovoltaic (PV) based home appliances [4] and [5]. One of the foremost challenges observed by the developing countries like India is the energy supply to far-flung areas. In lieu of this, the SPV air cooling system is designed which can be easily employed in remote and isolated areas for home appliances.

The PMDC motors are widely used in various applications due to its low cost construction, simple and inexpensive control and requirement of no external controller. But some of the flaws of the PMDC motor make it unsuitable for SPV array based appliances since at higher speeds, brush friction increases, thus reducing useful torque. Other demerits include higher armature reaction, lower speed range owing to mechanical limitations on the brushes, and since the field in the air gap is permanent and restricted, it cannot be controlled externally. In recent years, BLDC motors have gained popularity in a plethora of applications. The BLDC motor is far more dependable than the DC motor because it uses an electronic commutator instead of a mechanical commutator. The advantages of brushless motors over brushed DC motors include: better speed versus torque characteristics, high efficiency and reliability, noiseless operation, longer lifetime, eradication of ionizing sparks from the commutator and an altogether trimming of ElectroMagnetic Interference (EMI). Due to all above paramount advantages, BLDC

motor has been chosen to develop SPV fed air cooler [6] and [7].

Maximum efficiency of the SPV array is attained via a Maximum Power Point Tracking (MPPT) algorithm using the DC-DC converters [8]. Numerous DC-DC converters have been employed for MPPT in different SPV array based applications. However, most of the classical converter topologies have the highest values of reactive components resulting in an increased cost, size and weight and therefore, in the proposed system, a boost converter with desired features such as good switch utilization, high conversion efficiency, low stress on semiconductor devices and minimal number of reactive elements is selected [9], [10] and [6]. The SPV array is chosen such that its MPP always occurs within the bounded MPP region of the boost converter so that the power is invariably optimized immaterial of the variation in solar irradiance and loading conditions. Several non-identical MPPT algorithms have been recommended and the simplest one is to operate the PV array at constant voltage equal to the MPP voltage of the array [11] and [12]. Perturb & Observe (P&O) MPPT method is utilized in this paper because of its sharp fidelity of tracking even under the abrupt change in the environmental state. The perturbation size is prudently selected such that the oscillation around the peak point is prevented [13] and [14].

The structure of the paper is as follows: First section provides the introduction of the paper. Section 2. describes the various stages in the configuration of the conventional and the proposed system and Sec. 3. deals with the design of the PV array. Section 4. and Sec. 5. discuss about the design of DC-DC boost converter and Sinusoidal Pulse Width Modulation (SPWM) technique based inverter. Section 6. illustrates the BLDC motor drive system and Sec. 7. presents the control techniques of the system. Section 8. shows the results and the simulation work carried through MATLAB/Simulink and the final section exemplifies the conclusion.

2. Proposed System Description

The block diagram of the conventional PMDC motor based air cooling system and the proposed BLDC motor drive based air cooling system are depicted in Fig. 1 and Fig. 2 respectively.

In the conventional system, as shown in Fig. 1, the solar panel produces the required electrical power and feeds the DC-DC boost converter through the MPPT controller. The DC output power of the boost converter is utilized to energize the two PMDC motors to drive the centrifugal water pump and a fan blower. The
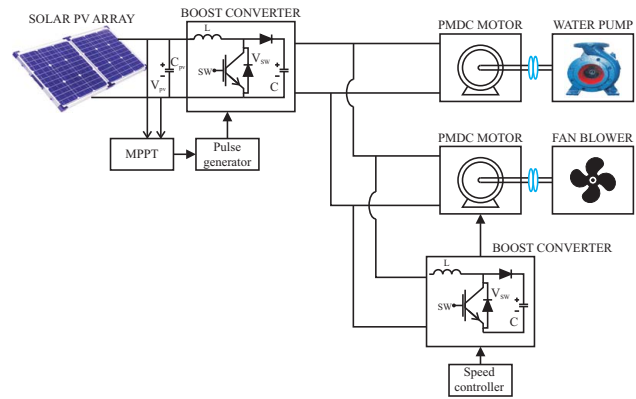

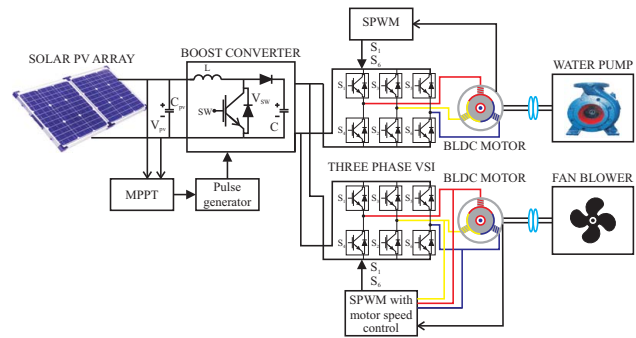**Fig. 1:** Conventional PMDC driven air cooling system.

Fig. 2: Proposed BLDC driven air cooling system.

speed of the fan blower is controlled through a speed controller and since MPPT and speed control cannot be achieved through one single converter, additional boost converter is utilized to the PMDC motor coupled to the fan blower.

In the proposed system, the SPV array output is fed to the DC-DC boost converter which is operated through the MPPT controller. The two VSI's converts the DC input power fed from the DC-DC converter to AC power to run the two BLDC motors coupled to the centrifugal water pump and a fan blower. The inbuilt encoder appended in the BLDC motor encodes the signal generated by the Hall sensors. These signals are converted by the encoder depending on the position of the rotor and accordingly gate pulses are generated to control the stator currents of the BLDC motor. The electronic commutator takes these signals and controls the gate pulses of the inverter. The speed of the fan blower coupled to one of the BLDC motor is controlled through a speed controller. As the BLDC motor VSI's operate at the fundamental frequency, the high frequency switching losses and the brush losses are eliminated, contributing to the reliable and high efficiency operation of the proposed air cooler system. The thorough design of various components at various stages such as SPV array, DC-DC boost converter, SPWM technique based inverter, PMDC motor, BLDC

motor, water pump and fan blower are described as follows.

3. Design of PV Array

The conversion of solar energy to electrical energy is done through solar PV cells. The equivalent circuit of a practical PV cell is shown in Fig. 3, which consists of a current source I_{ph}, a series resistance R_s and a parallel resistance R_{sh} [2]. For an ideal PV cell the parallel resistance is infinite and the series resistance is zero. Hence the output current of an ideal PV cell is given by the Eq. (1) and Eq. (2):

$$I_{pv} = I_{ph} - I_d - I_{sh}, \tag{1}$$

$$I_{pv} = I_{ph} - I_s e^{\left(\frac{qv}{kTA} - 1\right)} - \frac{V_{pv}}{R_{sh}}, \tag{2}$$

where I_s is the saturation current, q is the electron charge ($1.6 \cdot 10^{-19}$ (C)), k is Boltzmann constant ($1.38 \cdot 10^{-23}$ (J·K^{-1})), A is the diode ideality factor, T is the PV cell temperature (K).
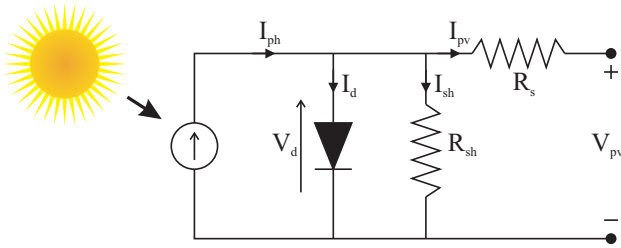

Fig. 3: PV cell equivalent circuit.

To increase the output voltage or the output current, the PV cells are connected in series or parallel combinations to form solar arrays [15]. Let N_s be the number of cells connected in series and N_p the number of cells connected in parallel, then the output current of an ideal PV cell is given by the Eq. (3) [16].

$$I_{pv} = N_p I_{ph} - N_p I_s \left(e^{\frac{qv}{N_s A k T}} - 1 \right). \tag{3}$$

The capacity of SPV array is selected slightly greater than the capacity of the PMDC and BLDC motors, which perpetuates the smooth functioning of the system despite the power losses. Hence, the selected capacity of SPV array is $P_{mpp} = 900$ W which is slightly more than what is required by the motors and also, all its parameters are framed accordingly. The voltage of the SPV array at MPP is selected considering BLDC motor voltage rating which is similar to the VSI DC link voltage rating. Table 1 summarizes the estimation of the various parameters to design an SPV array of appropriate size [6].

Tab. 1: Design of SPV array.

SPV Module	
Open circuit voltage, V_o (V)	44.5
Short circuit current, I_s (A)	8.83
Operating Temperature (°C)	30
Number of modules in a cell, N_{ss}	72
Series resisitance (Ω)	0.101
Parallel resistance (Ω)	1200
SPV Array	
Power at MPP, P_{mpp} (W)	900
Voltage at MPP, V_m (V)	108
Current at MPP, I_m (A)	8.83
Number of strings in series	3
Number of strings in parallel	1

4. Design of Boost Converter

SPV systems require the use of DC-DC converters to regulate and control the sporadic output of the solar panel. In addition, the boost converter topology is the only one that allows follow up of the PV array MPP notwithstanding the temperature, irradiance, and connected load [17] and [18]. The SPV array voltage at MPP, $V_{pv} = 108$ V appears as the input voltage source, whereas DC link voltage of VSI, $V_{dc} = 231$ V appears as the output voltage of the boost converter. The duty ratio D, of the boost converter is evaluated by employing the input-output relationship [14] as shown in Eq. (4):

$$D = \frac{V_{dc}}{V_{dc} + V_{pv}} = 0.6814. \tag{4}$$

The average current flowing through the DC link, I_{dc} is estimated by the Eq. (5):

$$I_{dc} = \frac{P_{mpp}}{V_{dc}} = 3.8961 \text{ A.} \tag{5}$$

The design calculations of inductor L and DC link capacitor C [6] are done as shown in Eq. (6) and Eq. (7):

$$L = \frac{D \cdot V_{pv}}{f_{sw} \cdot \Delta I_L} = 1.5 \text{ mH,} \tag{6}$$

$$C = \frac{I_{dc}}{6 \cdot \omega \cdot \Delta V_{dc}} = 3000 \text{ μF,} \tag{7}$$

where f_{sw} is the switching frequency of the boost converter, I_L is the average current flowing through the inductor, ΔI_L is the amount of ripple permitted in the current and ΔV_{dc} is ripple permitted in the voltage.

5. SPWM Technique Based Inverter

Inverter is the most important device to utilize the renewable energy sources efficiently. Also BLDC motors

makes use of inverters as electronic commutators to establish alternating current in congruent with the rotor position to produce the required torque. An equivalent circuit of a three phase SPWM technique based inverter utilized in the proposed system is demonstrated in Fig. 4. The main objective of the circuit is to generate a sinusoidal output voltage with tractable magnitude and frequency. For this, the switching signals are produced in such a way as to get the desired output. To generate the switching signals, a sinusoidal control signal of desired frequency is compared with a triangular waveform. According to the generated switching signals the inverter switches are controlled to get a three phase output voltage [19]. The Sinusoidal Pulse Width Modulation (SPWM) technique is one of the most popular techniques for harmonic reduction of inverters. In SPWM technique, three sine waves and a high frequency triangular carrier wave are used to generate PWM signal. Generally, three sinusoidal waves are used for three phase inverter. The sinusoidal waves are called reference signals and they have 120° phase difference with each other. The frequency of these sinusoidal waves is chosen based on the required inverter output frequency [8]. The three sinusoidal modulating signals should be balanced to get a balanced three phase output and also, it is important that the carrier waveform for all the three legs remains identical.
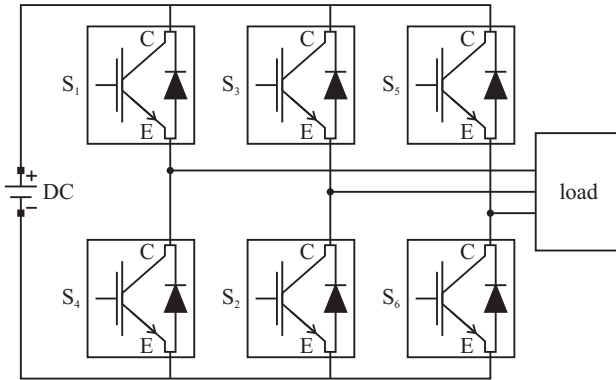

Fig. 4: Equivalent circuit of a three-phase inverter.

6. Design of the Proposed BLDC Motor Drive

6.1. Design of BLDC Motor

BLDC motors are considered to have various advantages [17], [18] and [19] and hence are used to develop a SPV fed air cooler, which can operate satisfactorily for longer time as compared to the PMDC motors under the dynamically changing atmospheric conditions.

Though PMDC motor is widely used in various applications, some of its drawbacks restrict its use in SPV array based appliances. This is because at higher speeds, brush friction increases, thus reducing useful torque. Other demerits include higher armature reaction, lower speed range owing to mechanical limitations on the brushes and since the field in the air gap is permanent and restricted it cannot be controlled externally. In view of this, BLDC drive system is deployed in the proposed work and its efficiency is compared with that of a PMDC drive system. It is shown that the former system gives high performance from the simulated results.

The voltage equations of the three windings of the BLDC motor are given by the Eq. (8), Eq. (9) and Eq. (10) [20], [21] and [22]:

$$V_a = Ri_a + L\frac{\mathrm{d}i_a}{\mathrm{d}t} + E_a, \tag{8}$$

$$V_b = Ri_b + L\frac{\mathrm{d}i_b}{\mathrm{d}t} + E_b, \tag{9}$$

$$V_c = Ri_c + L\frac{\mathrm{d}i_c}{\mathrm{d}t} + E_c, \tag{10}$$

where V_a, V_b and V_c are the phase voltages, i_a, i_b and i_c are the phase currents, E_a, E_b and E_c are the phase back-EMF, R is the phase resistance, L is the self inductance of the each phase.

The total output torque is the sum of the three torques in the three phases given by the Eq. (11):

$$\tau = \frac{E_a i_a + E_b i_b + E_c i_c}{\omega_r}, \tag{11}$$

where ω_r is the speed of the rotor.

The mechanical equation of the motor is given by the Eq. (12):

$$\tau - \tau_p - \tau_b = J\left(\frac{\mathrm{d}\omega}{\mathrm{d}t}\right) + \beta\omega, \tag{12}$$

where τ_p and τ_b are the pump load torque and blower load torque respectively, J is the rotor inertia, β is the friction constant (Nm·s·rad^{-1}).

Since the conventional drive circuits are expensive, bulky and complex, this paper proposes a low cost, compact, user friendly and high performance BLDC drive system which employs solar module. The practical converters undergo various power losses and the functioning of the BLDC motors is affected by the mechanical and electrical losses associated with them. To compensate these losses, the maximum power capacity of SPV array is selected slightly more than that of the BLDC motors which facilitates the flawless operation of the proposed system despite the power losses [18] and [19]. The parameters and ratings of the BLDC motor and the PMDC motor selected are indicated in the Tab. 2.

Tab. 2: Specifications of PMDC and BLDC motors.

Parameter	Value
Power P (W)	400
Speed, N (rpm)	1000
DC voltage, V_{dc} (V)	182
Current, I_s (A)	2.21
No. of poles P	4

6.2. Design of Water Pump

One of the BLDC motors is coupled to the water pump which is driven as a load to the BLDC motor by giving a load-torque signal depending on the torque-speed characteristic equation of a pump [15]. The rating of the pump is taken as 0.4 kW and the estimation of proportionality constant, K_p for the selected water pump is taken by its torque-speed characteristics Eq. (13):

$$K_p = \frac{\tau_p}{\omega_p^2} = \frac{P_p}{\omega_p^3} = 3.48 \cdot 10^{-4}, \qquad (13)$$

where ω_p is the mechanical speed of the rotor in rad·s^{-1}, τ_p is the electromagnetic torque developed and P_p is the rated power developed by the BLDC motor connected to the water pump under steady state for stable operation [23] and [24]. The detailed specifications of the centrifugal water pump are given in Tab. 3.

Tab. 3: SIMULINK parameters of water pump and air blower.

Parameter	Value
Number of Phases	3
Back EMF waveform	Trapezoidal
Stator Phase resistance R_s (Ω)	0.2
Stator phase inductance L_s (mH)	8.5
Flux linkage (V·s)	0.175
Voltage constant (V/K$_{rpm}$)	146.6077
Torque constant (N·m/A$_{peak}$)	1.4
Back EMF flat area in degrees	120
Inertia (Kg·m^2)	0.089
Friction (N-m-s)	0.005
Pole pairs	4

6.3. Design of Fan Blower

A fan blower is realised as a load to the second BLDC motor and its torque-speed characteristics is related with the Eq. (14):

$$K_b = \frac{\tau_b}{\omega_b^2} = \frac{P_b}{\omega_b^3} = 3.48 \cdot 10^{-4}, \qquad (14)$$

where, τ_p is the load torque offered by the blower which is equal to the electromagnetic torque developed by the BLDC motor under steady state for stable operation, ω_b is the mechanical speed of the rotor in rad·s^{-1} and P_b is the rated power developed by the BLDC motor

connected to the blower fan under steady state condition. The detailed specifications of the fan blower are given in Tab. 4.

7. Control Schemes of the Proposed System

The air cooling system proposed is controlled through three control schemes viz. MPPT, electronic commutation and DC-link voltage controller [17]. These schemes are detailed as follows:

7.1. P&O-MPPT Algorithm

The salient features of all solar panels include a distinct Maximum Power Point (MPP) and a nonlinear voltage-current characteristic, which relies on the atmospheric conditions, such as temperature and irradiance. In order to continuously harvest maximum power from the solar panels, they have to be operated at their MPP despite the inevitable changes in the environment. The solar to electrical energy conversion efficiency of solar cell lies between 9–20 %. Hence, it is important to use MPPT controller to enhance the overall efficiency of system [13], [14] and [9]. As per the maximum power transfer theorem, a source can deliver maximum power if the source and load impedance is same. Here DC-DC boost converter serves the purpose of impedance matching of source and load. To extract maximum possible power from a varying source, MPPT algorithms are used to match the source and the load properly. In this work, an efficient, simple and common P&O MPPT technique is utilized. The operating voltage is sampled and the algorithm changes the operating voltage by changing the duty ratio in the required direction depending on the sign of the difference between the samples of power and voltage as shown in Fig. 5.

This algorithm is not suitable when the variation in the solar irradiance is high. The voltage actually never reaches an exact value but perturbs around the MPP. Selecting an optimum value of perturbation size not only avoids the oscillations around the MPP but also reduces the starting current of the BLDC motor [25], [26] and [27]. An intellectual agreement between the tracking time and the perturbation size is also held to fulfill the required objectives [28].

7.2. Electronic Commutation

Electronic commutation of BLDC motors produces the switching signals for the VSI and decodes three Hall effect signals which are produced by an inbuilt encoder of the motor depending on the angular position
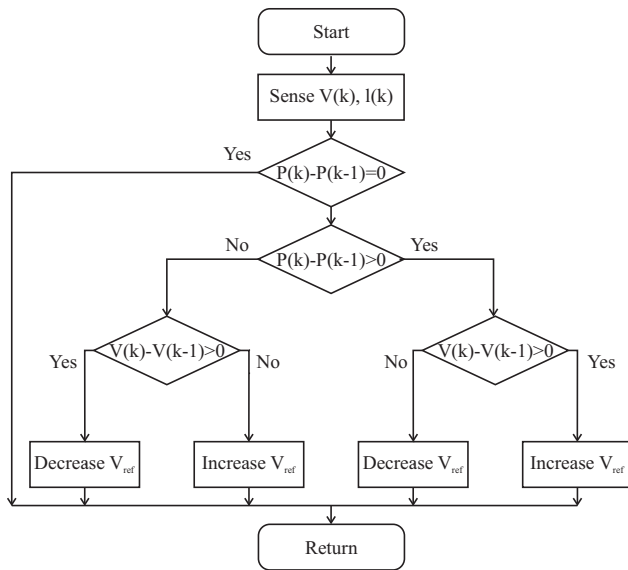
Fig. 5: Flow chart of P&O MPPT.

of the rotor. BLDC motors need to operate more efficiently to reduce the energy and save cost. Moreover, to ensure greater efficiency, the correct Hall-effect sensors need to be selected for electronic commutation. These Hall effect signals are logically converted into 6 switching pulses which are further used to operate the 6 IGBT switches of the VSI. Table 4 depicts the switching states of VSI for each set of Hall-effect signal states.

Tab. 4: Switching states for electronic commutation of BLDC Motor.

0°	Hall Signals			Switching States					
	H_1	H_2	H_3	S_1	S_2	S_3	S_4	S_5	S_6
NA	0	0	0	0	0	0	0	0	0
0-60	1	0	1	1	0	0	1	0	0
60-120	0	0	1	1	0	0	0	0	1
120-180	0	1	1	0	0	1	0	0	1
180-240	0	1	0	0	1	1	0	0	0
240-300	1	1	0	0	1	0	0	1	0
300-360	1	0	0	0	0	0	1	1	0
NA	1	1	1	0	0	0	0	0	0

For the fan blower, the hysteresis control method is used to obtain a preset speed. The reference speed when compared with the original speed of the BLDC motor, generates a torque reference which when divided by the constant K_b obtained from Eq. (4) gives the current reference magnitude. To get current reference, this current reference magnitude is multiplied with current pattern generated through the Hall signals. The three current references thus produced are then compared with the actual current flowing in the stator and the error signal is then made to pass through the Proportional Integral (PI) controller which then generates two pulses each. Hence, the 6 pulses gener-

ated are given to the gates of the VSI switches resulting in a desired speed of the BLDC motor [29] and [30].

The speed of the BLDC-motor for the water pump is regulated through the DC link voltage and the speed is fixed without using any external controlling circuit. Hence, by maintaining the power balance, it is ensured that the DC link voltage remains within limits [28] and [31].

7.3. DC-Link Voltage Controller

If only the air blower is to be operated and no controller is used, then the DC-link voltage increases gradually due to the lack of power balance. Hence to restrict this, the power balance (Generated power = Power consumed + Losses) should be maintained.
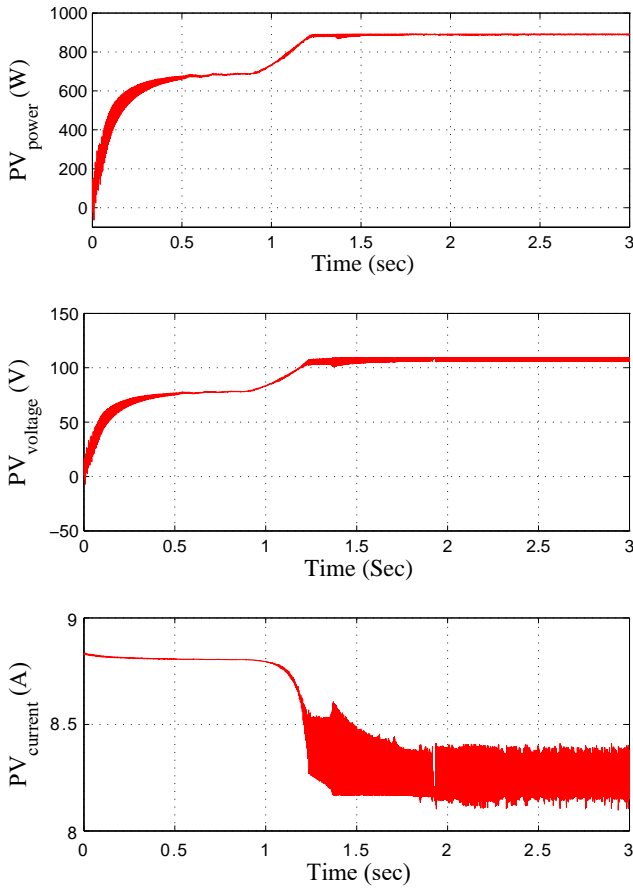
And the correct assessment of the losses is formidable. Now with the help of the DC-link voltage controller, the DC-link voltage is maintained; but this makes the SPV to be operated below MPP if the voltage reference to the DC-link voltage controller is other than Vmpp. Hence, less power is obtained. However, this will not give rise to a difficult condition as the mechanical load specified to be driven now is also diminished.

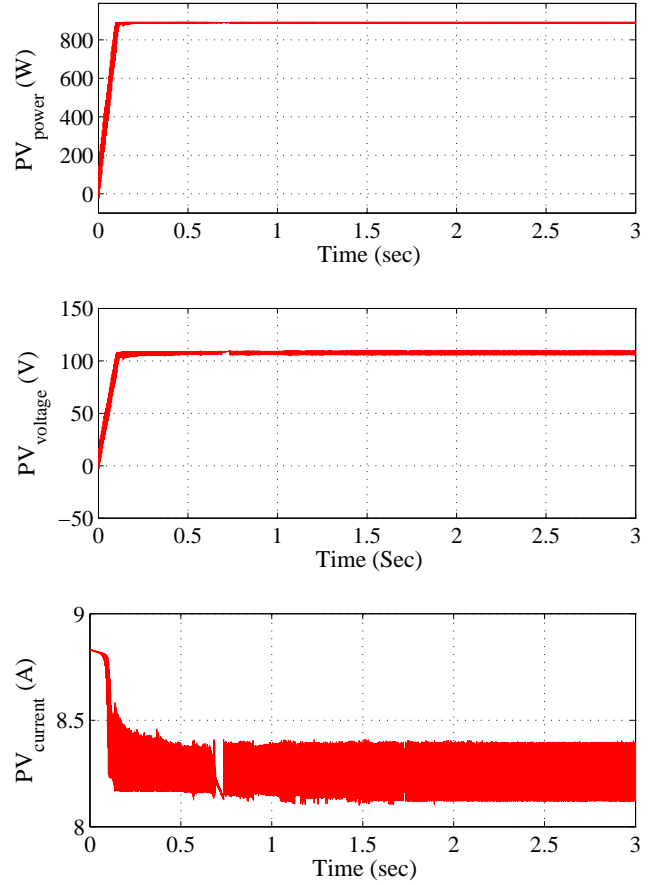## 8. Summary of Simulation Results

Performance evaluation of the proposed air cooler is carried out using simulated results in MATLAB/Simulink considering the starting and steady state condition at the standard solar irradiance of 1000 $W \cdot m^{-2}$ and 600 $W \cdot m^{-2}$ [6] and [7]. Further, the performance of BLDC motor is compared with a PMDC motor and the results are demonstrated on an individual basis in the following subsections.

8.1. Starting and Steady State Performances of PMDC Motor Drive System and BLDC Motor Drive System at Solar Irradiance of 1000 $W \cdot m^{-2}$

The parameters of SPV array, boost converter of the PMDC motor drive and BLDC motor drive connected to the two loads water pump and fan blower at a steady state solar irradiance of 1000 $W \cdot m^{-2}$ are exemplified in Fig. 6, Fig. 7, Fig. 8, Fig. 9, Fig. 10, Fig. 11 and Fig. 12, and detailed in the following subsections.

Fig. 6: PMDC motor output parameters of the PV at irradiance of 1000 W·m^{-2}.

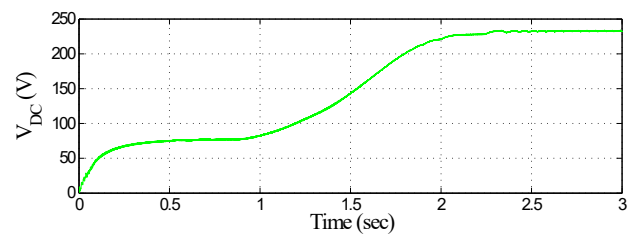**Fig. 7:** BLDC motor output parameters of the PV at irradiance of 1000 W·m^{-2}.

1) Performance of SPV Array at Steady State Irradiance of 1000 W·m^{-2}

The Fig. 6 and Fig. 7 shows the output parameters of the PV array viz; PV$_{power}$, PV$_{voltage}$ and PV$_{current}$ and the tracking performance of the P&O MPPT technique under the steady state condition of irradiance of 1000 W·m^{-2} of the PMDC motor and BLDC motor respectively. These indices correspond to the operation of the SPV array at MPP as PV power reaches 900 W at steady state.From the two figures, it can be illustrated that both the PMDC and BLDC motor's PV array output indices increase and reach their steady state values at the solar irradiance of 1000 W·m^{-2}.

2) Performance of Boost Converter at 1000 W·m^{-2}

The behaviour of the boost converter at 1000 W·m^{-2} for the PMDC motor and BLDC motor are shown in Fig. 8. where the DC link voltage is presented. It is inferred from waveforms that the converter operates in CCM, for both the motors resulting in a delimited strain on the components.The peak voltage on

the switch for both the motors is observed as 310 V but the steady state value is arrived at 2 seconds for the PMDC drive system and 0.5 seconds for the BLDC

(a) PMDC motor.

(b) BLDC motor.

Fig. 8: Output parameters of boost converter at irradiance of 1000 W·m^{-2}.

drive system. Moreover, in both the cases V_{dc} reaches the rated DC voltage.

3) Performance of PMDC Motor at Steady State Irradiance of 1000 W·m^{-2}

Performance of the PMDC motor at steady state irradiance of 1000 W·m^{-2} connected to the two loads motor fan and pump are shown in Fig. 9 and Fig. 10. The variables viz. the current, the torque, the speed and the output power when plotted against time reach their steady state values within 2 seconds which is slightly more than that of the BLDC motor. The starting current of BLDC motor is bounded within the permissible range and hence the motor has a soft start.

4) Performance of BLDC Motor at Steady State Irradiance of 1000 W·m^{-2}

The starting and steady state behaviours of the BLDC motor fan and motor pump at 1000 W·m^{-2} are shown in Fig. 11 and Fig. 12 and the following points are inferred from the simulation results. All the motor indices of the BLDC motor such as the stator current, the electromagnetic torque, the speed and the output power offered by fan and pump reach their rated values within 0.5 s under steady state condition as MPP is tracked whereas the PMDC motor parameters takes 2 seconds to reach their steady state values. The BLDC motor draws it's rated current and attain the rated speed, resulting in the water pumping and fan operating with full capacity. However, a minute and admissible pulsation in the electromagnetic torque is seen due to the electronic commutation in the DC link current of
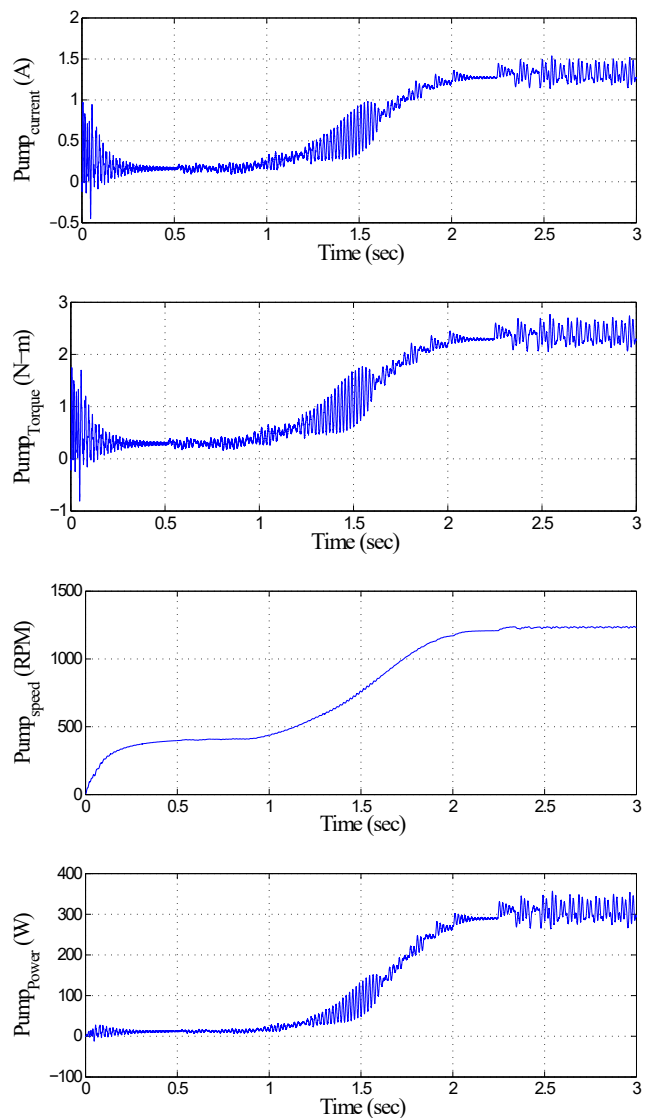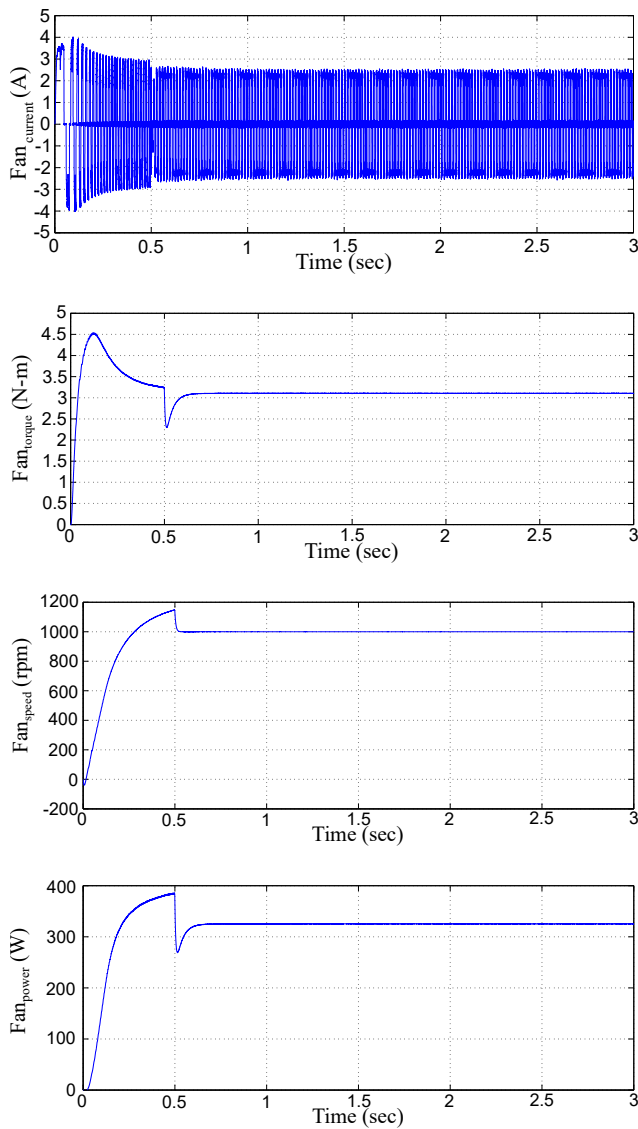

Fig. 9: PMDC-motor–fan blower parameters at irradiance of 1000 W·m^{-2}.

Fig. 10: PMDC-motor–pump parameters at irradiance of 1000 W·m^{-2}.
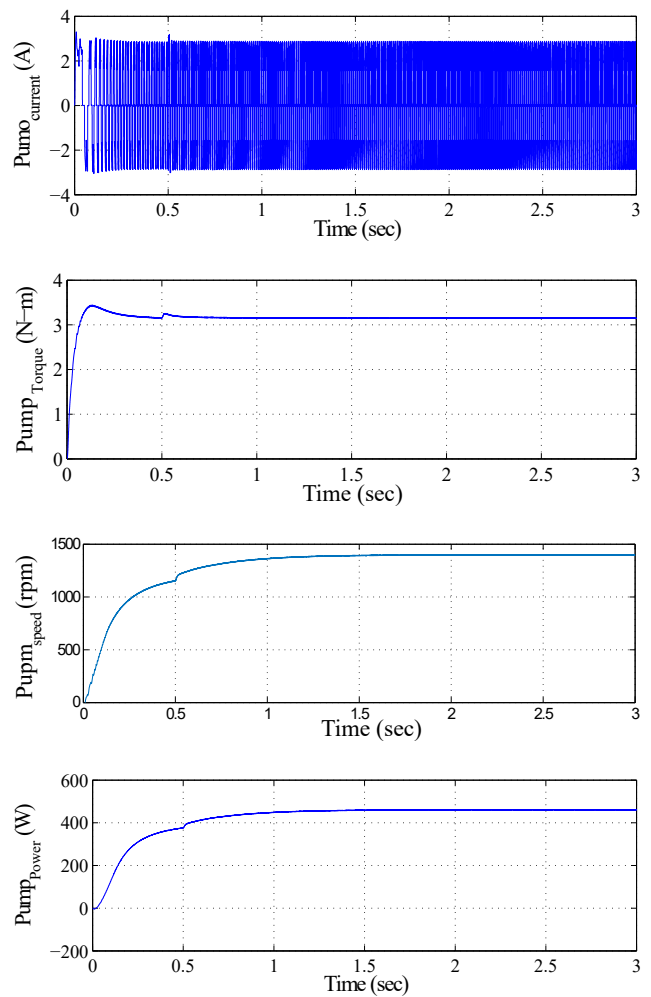
Fig. 11: BLDC-motor-fan blower parameters at irradiance of 1000 W·m^{-2}.

VSI. The starting current of BLDC motor is bounded within the the permissible range hence the motor has a soft start [17].

8.2. Starting and Steady State Performances of PMDC Motor Drive System and BLDC Motor Drive System at Solar Irradiance of 600 W·m^{-2}

The various performance indices of SPV array, boost converter and PMDC motor drive and BLDC motor drive under starting and steady state at the standard

Fig. 12: BLDC-motor-water pump parameters at irradiance of 1000 W·m^{-2}.

solar irradiance of 600 W·m^{-2} are illustrated in Fig. 13, Fig. 14, Fig. 15, Fig. 16, Fig. 17, Fig. 18 and Fig. 19, and elaborated in the following subsections.

1) Performance of SPV Array at Steady State Irradiance of 600 W·m^{-2}

The Fig. 13 and Fig. 14 shows the perfomance of the PMDC and BLDC motors output parameters of the PV array viz; PV$_{power}$, PV$_{current}$ and PV$_{voltage}$ and the tracking performance of the P&O MPPT technique under the steady state condition of irradiance of 600 W·m^{-2}. The three indices obtained correlate to the SPV array working at MPP as the PV output power reaches 270 W for the PMDC drive and reaches 510 W for the BLDC drive. The oscillation around the MPP can be averted by the suitable choice of the perturbation range.
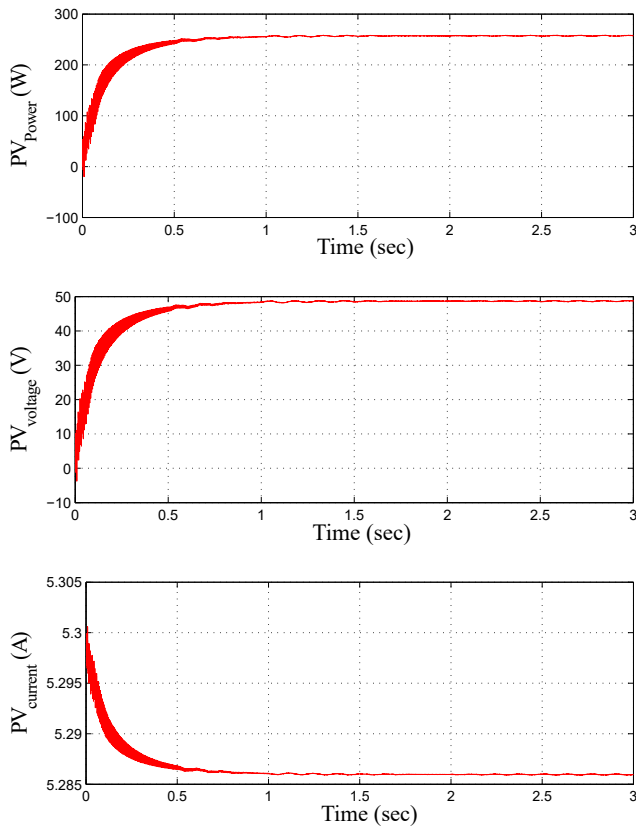
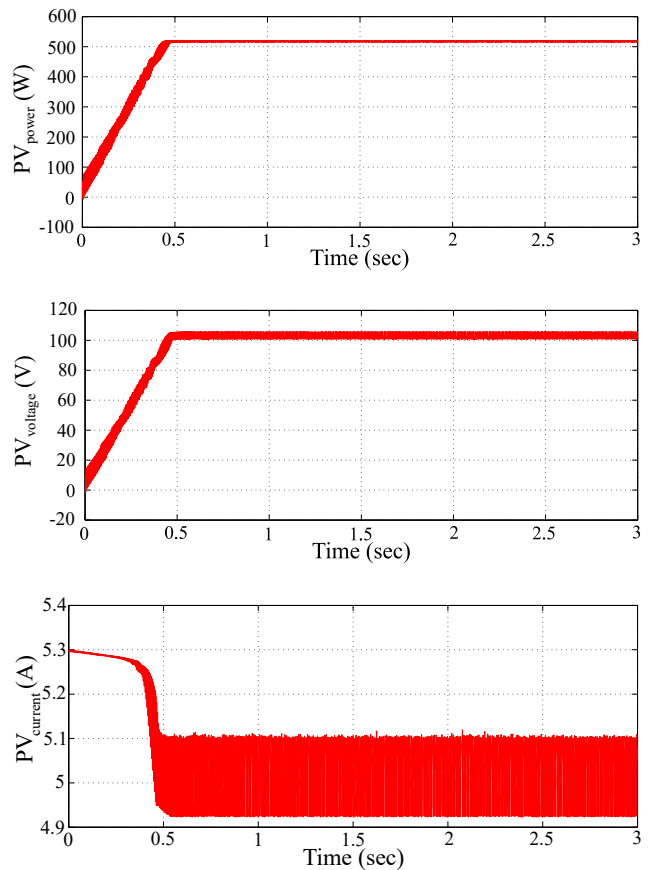**Fig. 13:** PMDC motor output parameters of the PV at irradiance of 6000 W·m^{-2}.

2) Performance of Boost Converter at 600 W·m^{-2}

The behaviour of the boost converter at 600 W·m^{-2} is shown in Fig. 15, where the DC link voltage of the PMDC and BLDC motor is presented. It is inferred from waveforms that the converter operates in CCM, irrespective of variation in solar irradiance. Also, at this irradiance, a DC voltage equal to 48 V for the PMDC motor and a DC voltage equal to 120 V for the BLDC motor sufficient to pump the water as well as to drive the fan blower is attained.
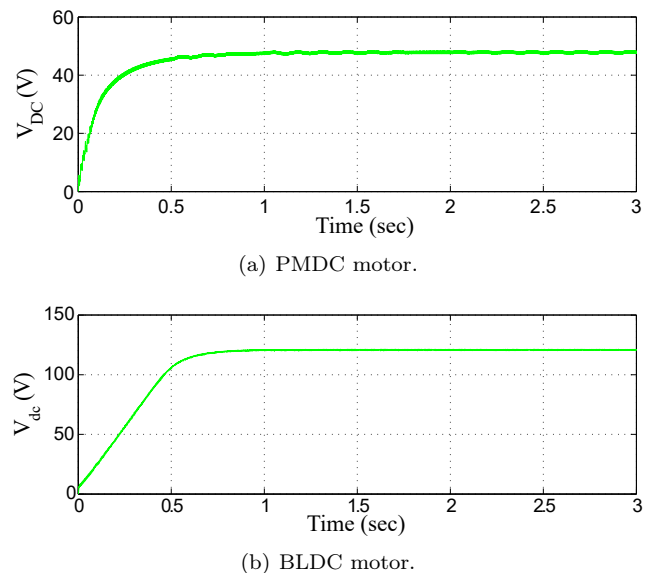

Fig. 14: BLDC motor Output parameters of the PV at irradiance of 6000 W·m^{-2}.

(a) PMDC motor.

(b) BLDC motor.

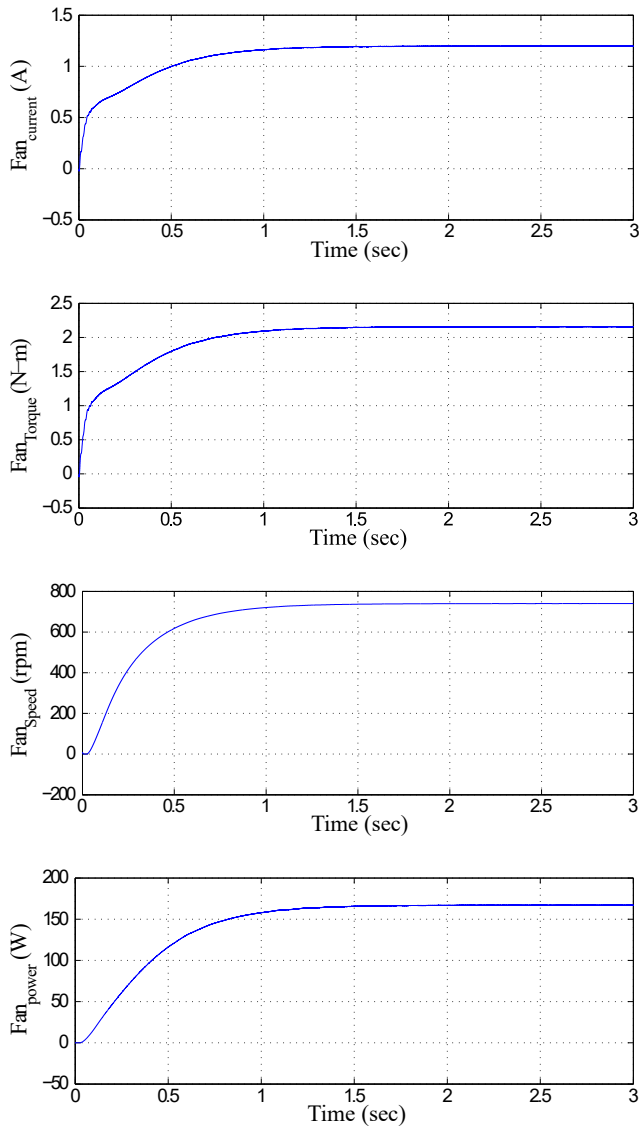**Fig. 15:** Output parameters of boost converter at irradiance of 6000 W·m^{-2}.

Fig. 16: PMDC-motor–fan blower parameters at irradiance of 600 W·m^{-2}.

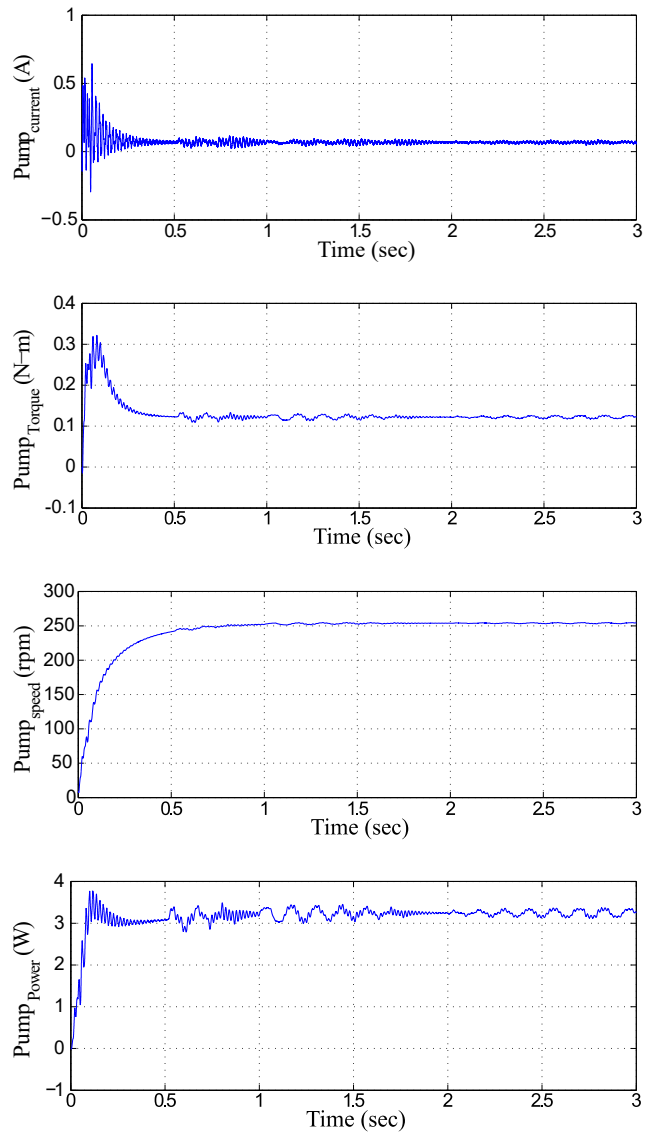**Fig. 17:** PMDC-motor–water pump parameters at irradiance of 600 W·m^{-2}.

3) Performance of PMDC Motor at Steady State Irradiance of 600 W·m^{-2}

Performance of the PMDC motor at irradiance of 600 W·m^{-2} for fan blower and motor pump are shown in Fig. 16 and Fig. 17. The variables viz. the stator current, the electromagnetic torque, the rotor speed and the output power are plotted against time. The PMDC motor attains a minimum speed of 780 rpm required to blow the fan whereas the pump speed is reduced to 260 rpm.

4) Performance of BLDC Motor at Steady State Irradiance of 600 W·m^{-2}

Performance of the BLDC motor for fan blower and motor pump at the irradiance of 600 W·m^{-2} are shown

in Fig. 18 and Fig. 19 and the following points are clearly observed from the presented simulation results. The variables viz. the stator current, the rotor speed, the electromagnetic torque and the output power offered by fan and pump reach their rated values within 0.5 s. Further, the motor attains a minimum speed of 700 rpm required to pump the water and drive the fan even at the irradiance of 600 W·m^{-2}. From the simulated results, it is seen that there is always torque balance between the BLDC motor and the loads irrespective of the solar irradiance. This torque balance between the BLDC motor and the loads irrespective of the solar irradiance variation verifies the stable operation of the proposed system.
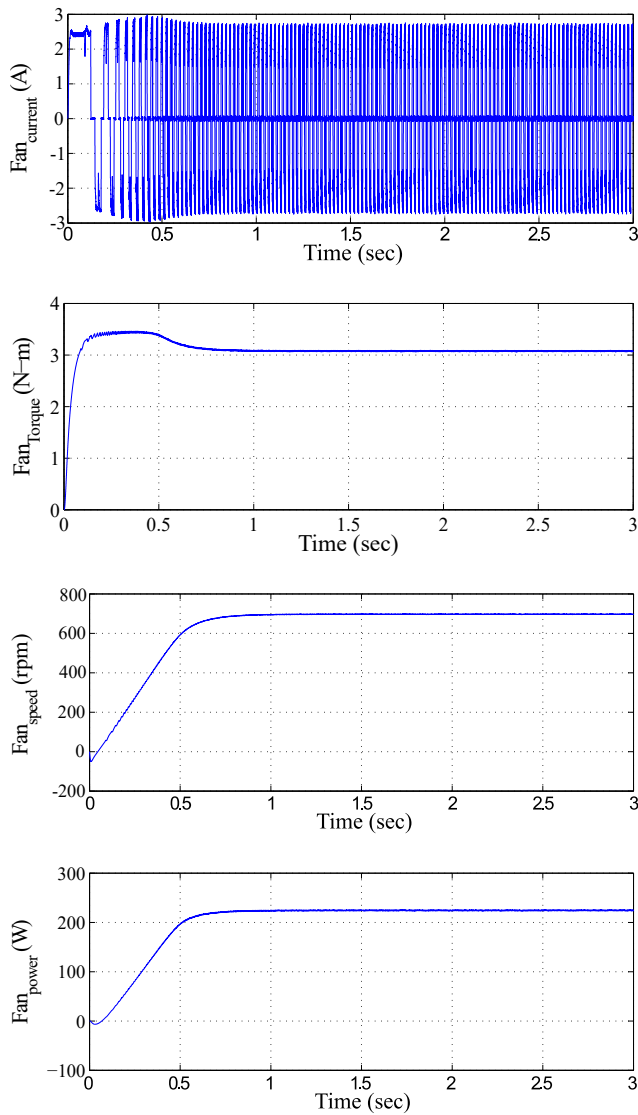
Fig. 18: BLDC-motor–fan blower parameters at irradiance of 600 W·m^{-2}.

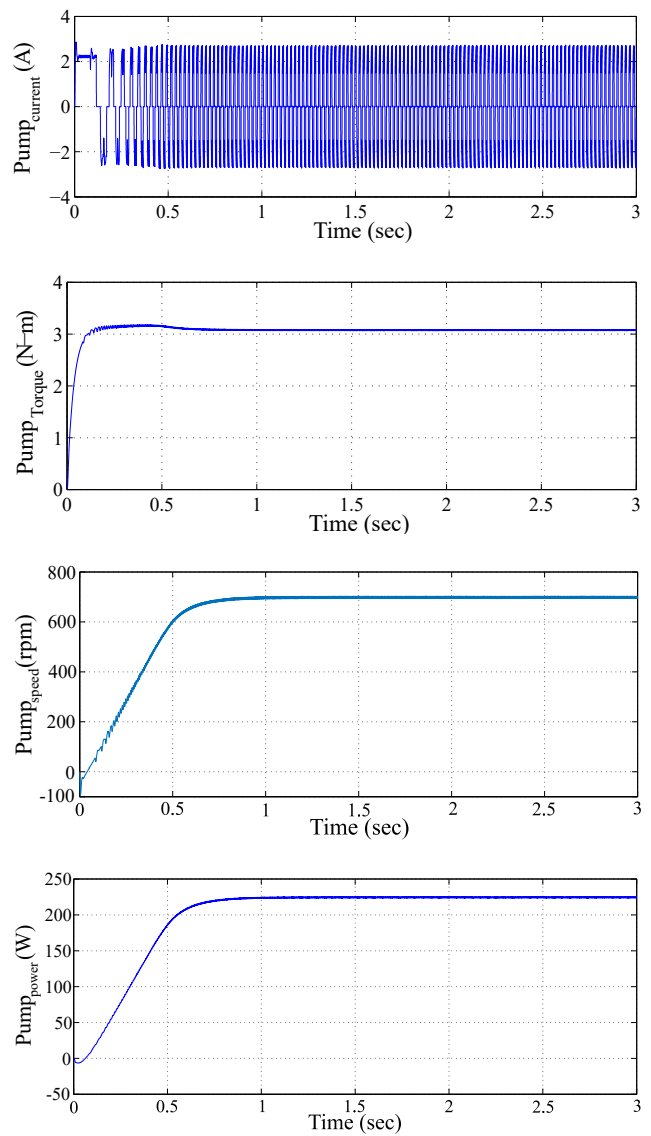**Fig. 19:** BLDC-motor–water pump parameters at irradiance of 600 W·m^{-2}.

8.3. Efficiency of PMDC Drive vs. BLDC Drive System

The efficiency evaluation of the proposed BLDC drive system and the PMDC drive system are shown in Tab. 5, subjected to the variation in irradiance, where η_D and η_B are the overall efficiences of the PMDC drive system and the BLDC drive system respectively. The graphical representation shown in Fig. 20, depicts the superior efficiency of the BLDC drive system over the PMDC drive system. It is observed from the efficiency values achieved that the BLDC drive attains an efficiency of 79.3 % at the minimum solar irradiance of 400 W·m^{-2} and as the irradiance increases beyond 600 W·m^{-2}, the efficiency of the system improves over 80 %, whereas the efficiency of the PMDC drive system varies between 60 % to 62 %, thus illustrating the advanced efficiency of the proposed BLDC system.
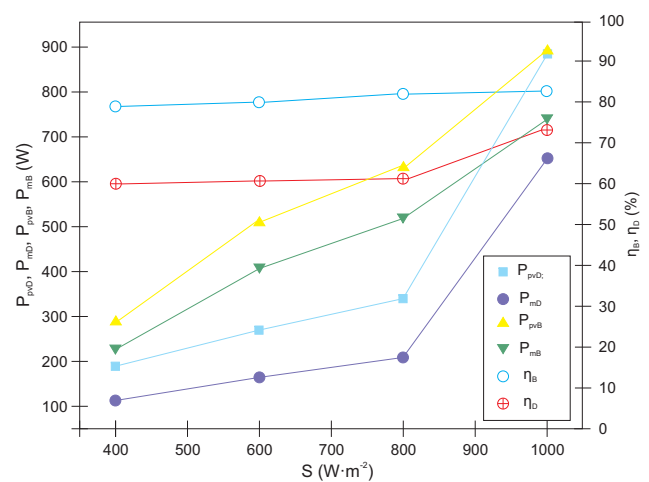

Fig. 20: Efficiency evaluation of proposed system.

Tab. 5: Efficiency evaluation of proposed system.

S (W·m^{-2})	PMDC driver output power			Proposed BLDC Drive System		
	P_{pvD} (W)	P_{mD} (W)	η_D (%)	P_{pvB} (W)	P_{mB} (W)	η_B (%)
400	190	115	60.5	290	230	79.3
600	270	165	61.1	510	410	80.3
800	340	210	61.7	630	520	82.5
1000	880	650	73.8	890	740	83.1

S: Irradiance.
P_{pvD}: PV output power of PMDC drive.
P_{mD}: PMDC drive output power.
η_D: Efficiency of PMDC drive.
P_{pvB}: PV output power of BLDC drive.
P_{mB}: Proposed BLDC drive output power.
η_B: Efficiency of proposed BLDC drive.

9. Conclusion

The main aim of the proposed system is to attain comfort level during summer for the people living in the rural areas where it is difficult to depend on the electricity for all the time. The performance analysis has demonstrated with the novel features of proposed system such as proper design of SPV array, MPPT with boost converter, speed control of BLDC motor by variable DC link voltage and soft starting of the motor by wisely tracking the MPP and electronic commutation with fundamental frequency switching. The boost converter, having the advantage of very good conversion efficiency is found to be more suitable for the proposed air cooling system. The MATLAB/Simulink based simulation results of BLDC drive displays superior outputs than the PMDC drive thus exhibiting the suitability of the BLDC drive system for the proposed system, regardless of the environmental conditions.

References

[1] BIALASIEWICZ, J. T. Renewable Energy Systems With Photovoltaic Power Generators: Operation and Modeling. *IEEE Transactions on Industrial Electronics*. 2008, vol. 55, iss. 7, pp. 2752–2758. ISSN 0278-0046. DOI: 10.1109/TIE.2008.920583.

[2] TIANZE, L., L. HENGWEI, J. CHUAN, H. LUAN and Z. XIA. Application and design of solar photovoltaic system. In: *3rd International Photonics & OptoElectronics Meetings*. Wuhan: IOP Publishing, 2010, pp. 1–6. ISBN 978-1617826603. DOI: 10.1088/1742-6596/276/1/012175.

[3] JAIN, S., A. K. THOPUKARA, R. KARAMPURI and V. T. SOMASEKHAR. A Single-stage photovoltaic system for a dual-inverter-fed open-end winding induction motor drive for pumping applications. *IEEE Transactions on Power Electronics*. 2015, vol. 30, iss. 9, pp. 4809–4818. ISSN 0885-8993. DOI: 10.1109/TPEL.2014.2365516.

[4] AN, L. and D. D. C. LU. Design of a Single-Switch DC/DC Converter for a PV-Battery-Powered Pump System With PFM+PWM Control. *IEEE Transactions on Industrial Electronics*. 2015, vol. 62, iss. 2, pp. 910–921. ISSN 0278-0046. DOI: 10.1109/TIE.2014.2359414.

[5] MAPURUNGA CARACAS, J. V., G. DE CARVALHO FARIAS, L. F. MOREIRA TEIXEIRA and L. A. DE SOUZA RIBEIRO. Implementation of a high-efficiency, high-lifetime, and low-cost converter for an autonomous photovoltaic water pumping system. *IEEE Transactions on Industry Applications*. 2014, vol. 50, iss. 1, pp. 631–641. ISSN 0093-9994. DOI: 10.1109/TIA.2013.2271214.

[6] KUMAR, R. and B. SINGH. BLDC Motor Driven Water Pump Fed by Solar Photovoltaic Array Using Boost Converter. In: *Annual IEEE India Conference (INDICON)*. New Delhi: IEEE, 2015, pp. 1–6. ISBN 978-1-4673-7399-9. DOI: 10.1109/INDICON.2015.7443676.

[7] KUMAR, R. and B. SINGH. Buck-boost converter fed BLDC motor drive for solar PV array based water pumping. In: *IEEE International Conference on Power Electronics, Drives and Energy Systems*. Mumbai: IEEE, 2014, pp. 1–6. ISBN 978-1-4799-6372-0. DOI: 10.1109/PEDES.2014.7042001.

[8] RASHID, M. H. *Power Electronics Handbook: Devices, Circuits, and Applications*. 3rd ed. Burlington: Elsevier, 2011. ISBN 978-0-12-382036-5.

[9] MAMARELIS, E., G. PETRONE and G. SPAGNUOLO. Design of a sliding-mode-controlled SEPIC for PV MPPT applications. *IEEE Transactions on Industrial Electronics*. 2014, vol. 61, iss. 7, pp. 3387–3398. ISSN 0278-0046. DOI: 10.1109/TIE.2013.2279361.

[10] TAGHVAEE, M. H., M. A. M. RADZI, S. M. MOOSAVAIN, H. HIZAM and M. HAMIRUCE MARHABAN. A current and future study on non-isolated DC-DC converters for photovoltaic applications. *Renewable and Sustainable Energy Reviews.* 2013, vol. 17, iss. 1, pp. 216–227. ISSN 1364-0321. DOI: 10.1016/j.rser.2012.09.023.

[11] ESRAM, T. and P. L. CHAPMAN. Comparison of photovoltaic array maximum power point tracking Techniques. *IEEE Transactions on Energy Conversion.* 2007, vol. 22, iss. 2, pp. 439–449. ISSN 0885-8969. DOI: 10.1109/TEC.2006.874230.

[12] SUBUDHI, B. and R. PRADHAN. A Comparative Study on Maximum Power Point Tracking Techniques for Photovoltaic Power Systems. *IEEE Transactions on Sustainable Energy.* 2013, vol. 4, iss. 1, pp. 89–98. ISSN 1949-3029. DOI: 10.1109/TSTE.2012.2202294.

[13] AASHOOR, F. A. O. and F. V. P. ROBINSON. Maximum power point tracking of photovoltaic water pumping system using fuzzy logic controller. In: *48th International Universities' Power Engineering Conference.* Dublin: IEEE, 2013, pp. 1–5. ISBN 978-1-4799-3254-2. DOI: 10.1109/UPEC.2013.6714969.

[14] ALGAZAR, M. M., H. AL-MONIER, H. ABD EL-HALIM and M. E. EL KOTB SALEM. Maximum power point tracking using fuzzy logic control. *International Journal of Electrical Power & Energy Systems.* 2012, vol. 39, iss. 1, pp. 21–28. ISSN 0142-0615. DOI: 10.1016/j.ijepes.2011.12.006.

[15] OUADA, M., M. S. MERIDJET and N. TALBI. Optimization photovoltaic pumping system based BLDC using fuzzy logic MPPT control. In: *International Renewable and Sustainable Energy Conference.* Ouarzazate: IEEE, 2013, pp. 27–31. ISBN 978-1-4673-6373-0. DOI: 10.1109/IRSEC.2013.6529718.

[16] ZAHAB, E. E. A., A. M. ZAKI and M. M. EL-SOTOUHY. Design and control of a standalone PV water pumping system. *Journal of Electrical Systems and Information Technology.* 2016, vol. 4, iss. 2, pp. 231–237. ISSN 2314-7172. DOI: 10.1016/j.jesit.2016.03.003.

[17] KUMAR, R. and B. SINGH. BLDC motor driven solar PV array fed water pumping system employing zeta converter. In: *IEEE India International Conference on Power Electronics.* Kurukshetra: IEEE, 2014, pp. 1–6. ISBN 978-1-4799-6045-3. DOI: 10.1109/IICPE.2014.7115771.

[18] UNO, M. and A. KUKITA. Single-switch voltage equalizer using multistacked buck–boost converters for partially-shaded photovoltaic modules. *IEEE Transactions on Power Electronics.* 2015, vol. 30, iss. 6, pp. 3091–3105. ISSN 0885-8993. DOI: 10.1109/TPEL.2014.2331456.

[19] MOZAFFARI NIAPOUR, S. A. K. H., S. DANYALI, M. B. B. SHARIFIAN and M. R. FEYAZI. Brushless dc motor drives supplied by PV power system based on Z-source inverter and FL-ICMPPT controller. *Energy Conversion and Management.* 2011, vol. 52, iss. 8–9, pp. 3043–3059. ISSN 0196-8904. DOI: 10.1016/j.enconman.2011.04.016.

[20] PILLAY, P. and R. KRISHNAN. Modeling, simulation, and analysis of permanent-magnet motor drives. Part II: The brushless DC motor-drive. *IEEE Transactions on Industry Applications.* 1989, vol. 25, iss. 2, pp. 274–279. ISSN 0093-9994. DOI: 10.1109/28.25542.

[21] SANITA, C. S. and J. T. KUNCHERIA. Modelling and simulation of four quadrant operation of three phase brushless DC motor with hysteresis current controller. *International Journal of Advanced Research in Electrical, Electronics and Instrumentation Engineering.* 2013, vol. 2, iss. 6, pp. 2461–2470. ISSN 2320-3765.

[22] PUTTA SWAMY, C. L. and B. P. SINGH. Dynamic performance of a permanent magnet brushless DC motor powered by a PV array forwater pumping. *Solar Energy Materials and Solar Cells.* 1995, vol. 36, iss. 2, pp. 187–200. ISSN 0927-0248. DOI: 10.1016/0927-0248(94)00174-Q.

[23] DURSUN, M. and S. OZDEN. Application of solar powered automatic water pumping in Turkey. *International Journal of Electrical and Computer Engineering.* 2012, vol. 4, no. 2, pp. 161–164. ISSN 2088-8708. DOI: 10.7763/IJCEE.2012.V4.471.

[24] TERKI, A., A. MOUSSI, A. BETKA and N. TERKI. An improved efficiency of fuzzy logic control of PMBLDC for PV pumping system. *Applied Mathematical Modelling.* 2012, vol. 36, iss. 3, pp. 934–944. ISSN 0307-904X. DOI: 10.1016/j.apm.2011.07.042.

[25] KOU, Y., Y. XIA and Y. YE. Fast variable step-size maximum power point tracking method for photovoltaic systems. *Journal of Renewable and Sustainable Energy.* 2015, vol. 7, iss. 4, pp. 1–16. ISSN 1941-7012. DOI: 10.1063/1.4928519.

[26] GOLDVIN SUGIRTHA DHAS, B. and S. N. DEEPA. Fuzzy logic based dynamic sliding mode

control of boost inverter in photovoltaic application. *Journal of Renewable and Sustainable Energy.* 2015, vol. 7, iss. 4, pp. 1–19. ISSN 1941-7012. DOI: 10.1063/1.4928737.

[27] ELTAMALY, A. M. Performance of smart maximum power point tracker under partial shading conditions of photovoltaic systems. *Journal of Renewable and Sustainable Energy.* 2015, vol. 7, iss. 4, pp. 1–16. ISSN 1941-7012. DOI: 10.1063/1.4929665.

[28] BENCHERIF, M. and A. CHERMITTI. New method to assess the loss parameters of the photovoltaic modules. *Journal of Renewable and Sustainable Energy.* 2012, vol. 4, iss. 6, pp. 1–19. ISSN 1941-7012. DOI: 10.1063/1.4767812.

[29] KUMAR DASH, S., S. NEMA, R. K. NEMA and D. VERMA. A comprehensive assessment of maximum power point tracking techniques under uniform and non-uniform irradiance and its impact on photovoltaic systems: A review. *Journal of Renewable and Sustainable Energy.* 2015, vol. 7, iss. 6, pp. 1–28. ISSN 1941-7012. DOI: 10.1063/1.4936572.

[30] CHO, H. Y., J. HYUN KIM, K. JONG LEE, S. HYON LEE and N. PARK. Network analysis of photovoltaic-related Science Citation Index papers in Korea. *Journal of Renewable and Sustainable Energy.* 2015, vol. 7, iss. 6, pp. 1–12. ISSN 1941-7012. DOI: 10.1063/1.4938148.

[31] ROGER, J. A. Theory of the direct coupling between D. C. Motors and photovoltaic solar arrays. *Solar Energy.* 1979, vol. 23, iss. 3, pp. 193–198. ISSN 0038-092X. DOI: 10.1016/0038-092X(79)90157-9.

About Authors

Shobha Rani DEPURU received her B.Tech. degree in Electrical and Electronics Engineering from Jawaharlal Nehru Technological University (JNTU), Hyderabad, India and the M.Tech degree in Electrical Power Systems from JNTU, Ananthapur, India and currently pursuing Ph.D. in the Department of Electrical and Electronics Engineering, Sri Venkateswara University College of Engineering, Tirupati, India. Her research interests are renewable energy sources, power system optimization, artificial intelligence techniques and power system reliability.

Muralidhar MAHANKALI received his B.Tech. degree in Electrical Engineering and the M.Tech degree in Instrumentation & Control systems from the Sri Venkateswara University College of Engineering, Tirupati, India, and the Ph.D. degree from Sri Venkateswara University College of Engineering, Tirupati, India. He is currently a Professor of Electrical Engineering in Sri Venkateswara College of Engineering and Technology, Tirupati, India. He published more than 70 research papers. So far, he has guided 9 Ph.D., and 38 M.Tech. students. His research interests include electrical engineering, instrumentation & control systems and High Voltage Engineering.